Predicting turbulence in flows with strong stable stratification

David A. Hebert and Stephen M. de Bruyn Kops
University of Massachusetts, Amherst, Amherst, Massachusetts 01003

(Received 23 August 2005; accepted 13 April 2006; published online 16 June 2006)

High resolution direct numerical simulations are used to understand how turbulence can be predicted in flows subject to strong stable stratification. It is observed that shear instabilities are the predominant cause of turbulence in the simulations, which supports the derivation of a Froude-Reynolds number scaling to predict turbulence in this flow regime. It is found that when the autocorrelation length of the horizontal velocities is used as the length scale for the Froude and Reynolds number then that length scale, the Froude number, and the Reynolds number all evolve, as theory suggests. An advection length scale based on the kinetic energy and its dissipation rate is found not to be of practical use for characterizing the flow. Finally, it is observed the Froude-Reynolds number parameter of Riley and de Bruyn Kops is very similar to the commonly used buoyancy Reynolds number. This suggests that a shear-based approach to parametrizing turbulence under stable stratification, rather than the ratio-of-length-scales approach that is often used as the physical justification for the buoyancy Reynolds number, might be appropriate. While the Froude-Reynolds parameter and the buoyancy Reynolds number are closely related, the former may be the more useful when configuring laboratory experiments or numerical simulations since it can be estimated *a priori*. © *2006 American Institute of Physics*. [DOI: 10.1063/1.2204987]

I. INTRODUCTION

When density is constant, predicting whether a flow will be laminar or turbulent can usually be done on the basis of the Reynolds number. Thus, when a laboratory experiment or direct numerical simulation is conducted with a Reynolds number that is high compared with that at which the flow transitions to turbulence, the results are often accepted as indicative of flows at very high Reynolds number. In the presence of stable stratification, however, predicting if a flow will be turbulent is more complicated in several ways. First, turbulence often occurs in intermittent patches, even at extremely high Reynolds numbers that occur in the ocean and atmosphere. The question becomes not only whether the flow is laminar or turbulent but also if turbulence will likely be important in the flow (e.g., as a mechanism for mixing). Second, stratification introduces a gravitational force to the flow, which, together with the viscous force, counters any tendency of the flow to be turbulent. In this context, the gravitational force is usually parametrized in the form of a Froude number, and physical reasoning suggests that turbulence will occur in some region of the Reynolds number-Froude number parameter space rather than simply when the Reynolds number is above some critical value. Thus, predicting when the results of a laboratory experiment or direct numerical simulation can be expected to be indicative of stably stratified geophysical flows is somewhat more difficult than predicting when the results from experiments in unstratified flows will scale up to higher Reynolds numbers.

The most common approach to assessing the importance of turbulence in stably stratified flows is to consider the buoyancy Reynolds number, $\mathrm{Re}_b=\epsilon/\nu N^2$, where ϵ is the kinetic energy dissipation rate, ν is the kinematic viscosity, and N is the buoyancy frequency (e.g., Refs. 1–4). Re_b can be derived from the ratio of the Ozmidov scale, $L_\mathrm{O}=(\epsilon/N^3)^{1/2}$, and the Kolmogorov scale, $L_\mathrm{K}=(\nu^3/\epsilon)^{1/4}$:

$$\mathrm{Re}_b=\left(\frac{L_\mathrm{O}}{L_\mathrm{K}}\right)^{\frac{4}{3}}=\frac{\epsilon}{\nu N^2}. \tag{1}$$

The physical justification for using Re_b as a measure of turbulence is based on what Gregg[2] refers to as a "bandwidth of length scales available to turbulence," i.e., Re_b, is the ratio of the maximum length at which eddies can overturn before being inhibited by buoyancy to the length scale at which overturning is precluded by viscous forces. According to this definition, for one decade of length scales to be available for turbulence to form, $\mathrm{Re}_b=21.5$. Gibson,[1] assuming isotropic turbulence and a transition to turbulence at Richardson number 1/4, found $\mathrm{Re}_b\approx 30$ for active turbulence to form. This value of Re_b is supported experimentally by Stillinger.[5] Shih *et al.*[6] compare several common overturning length scales to the Ellison scale for $0.1<\mathrm{Re}_b<1000$, demonstrating ranges of applicability for each length scale examined.

Recently, another approach to predicting turbulence in stratified flows was introduced by Riley and de Bruyn Kops.[7] Based on published laboratory and simulation results, in addition to those from their own simulations, they observe that in stratified wakes with no energy input from the mean flow, "pancake" eddies form that are weakly coupled in the vertical direction. High shear between these eddies can lead to Kelvin-Helmholtz instabilities, which, in turn, can trigger turbulence. By relating the Richardson number in these shear regions to Froude and Reynolds numbers (F_h and Re_h) based on the horizontal length scale, L_h, and the rms horizontal velocity, u_h, they conclude that turbulence can be expected to occur due to shear instabilities if $F_h^2\,\mathrm{Re}_h>\mathcal{O}(1)$.

The $F_h^2\,\mathrm{Re}_h$ scaling has several features that potentially make it attractive when compared with Re_b. First, for those designing numerical or laboratory experiments, it provides an *a priori* method for estimating if the results from the proposed experiments might be expected to scale up to the geophysical case before actually running the experiment in order to determine ϵ. Second, it provides an alternative physical justification for turbulence parametrization (i.e., shear instabilities) in contrast to the commonly used justification for Re_b, based on the ratio of length scales. Third, it involves two dimensionless groups, as predicted by dimensional analysis. It is not immediately clear, however, whether the Riley and de Bruyn Kops scaling is fundamentally different from the buoyancy Reynolds number or if they simply provided an alternative physical explanation for why Re_b is a useful turbulence parameter. A reason to suspect that $F_h^2\,\mathrm{Re}_h$ and Re_b may be related quantities is that the latter can also be written as the product of a Reynolds number and the square of a Froude number, both defined in terms of the advective length scale u^3/ϵ.[6,8]

In this paper we investigate $F_h^2\,\mathrm{Re}_h$ as a parameter for predicting turbulence in numerical simulations of a late wake. In the process, several definitions are considered for the length scale, L_h, including u_h^3/ϵ. We also compare $F_h^2\,\mathrm{Re}_h$ and Re_b for the simulated flows. Before presenting the analysis in Sec. IV, we discuss the numerical simulation methodology and give an overview of the simulation database in Secs. II and III.

II. METHODOLOGY

The simulated flows analyzed in this study are idealizations of that which results when a rake is dragged through a continuously stratified tank (e.g., Ref. 9), except with unity Schmidt number. In particular, there is no ambient shear and the stratification is constant in time. The simulations are discussed in detail in Ref. 7. Briefly, the initial condition consisted of Taylor-Green vortices plus broadbanded noise with a level approximately 10% of the Taylor-Green vortex energy. The Taylor-Green vortices satisfied the following mathematical form:

$$\mathbf{v_{tg}} = \mathcal{U}\cos(\kappa z)[\cos(\kappa x)\sin(\kappa y), -\sin(\kappa x)\cos(\kappa y), 0]$$

where $\mathcal{U}$ determines the initial velocity scale and $\ell = 1/\kappa$ determines the length scale for this field. Thus, for all simulation results, velocities are nondimensionalized by $\mathcal{U}$, lengths by $\ell = 1/\kappa$, and time by $\ell/\mathcal{U}$. The Froude number and Reynolds number characterizing the simulations are defined, respectively, as

$$F_L = \frac{2\pi\mathcal{U}}{N\ell}, \quad \mathrm{Re}_L = \frac{\mathcal{U}\ell}{\nu}. \tag{2}$$

The flow fields are assumed to satisfy the incompressible continuity and Navier-Stokes equations subject to the Boussinesq approximation. Using the nondimensionalization outlined previously, the governing equations are

$$\nabla\cdot\mathbf{v} = 0, \tag{3a}$$

$$\frac{\partial\mathbf{v}}{\partial t} + \mathbf{v}\cdot\nabla\mathbf{v} = -\left(\frac{2\pi}{F_L}\right)^2\rho\mathbf{e}_z - \nabla p + \frac{1}{\mathrm{Re}_L}\nabla^2\mathbf{v}, \tag{3b}$$

$$\frac{\partial\rho}{\partial t} + \mathbf{v}\cdot\nabla\rho - w = \frac{1}{\mathrm{Re}_L\,\mathrm{Sc}}\nabla^2\rho. \tag{3c}$$

Here $\mathbf{v}=(u,v,w)$ is the velocity vector and ρ and p are the density and pressure deviations from their ambient values. Also, $\mathrm{Sc}=\nu/\mathcal{D}$ is the Schmidt number with ν the kinematic viscosity and $\mathcal{D}$ the mass diffusivity, and $\mathbf{e}_z$ is a unit vector in the vertical (z) direction. The pressure has been scaled by the dynamic pressure, $\rho\mathcal{U}^2$, and the density scaled using the ambient density gradient (i.e., it is scaled by $\ell|d\bar{\rho}/dz|$).

A pseudospectral technique was used to compute the spatial derivatives, and a third-order Adams-Bashforth scheme with projection was used to advance the solution in time. A spherical wavenumber truncation of approximately 15/16, $\kappa_{\max}$, with $\kappa_{\max}$, the maximum wavenumber in the discrete Fourier transforms, was used to eliminate the most damaging aliasing errors. The momentum equation was advanced in time with the nonlinear term expressed in vorticity form, while the alternating time-step scheme suggested by Kerr[10] was employed for the density field to approximate the skew-symmetric form of the nonlinear term and thereby minimize aliasing.[11]

TABLE I. Conditions for simulations of quasihorizontal vortices. N_x, N_y, and N_z are the number of grid points in each direction.

Notation	F_L	Re_L	Pr	$\langle\mathrm{Re}_b\rangle_h$	N_x	N_y	N_z
F2R2	2	200	1	0.097	256	256	128
F2R4	2	400	1	0.22	256	256	128
F2R8	2	800	1	0.41	256	256	128
F2R16	2	1600	1	1.1	256	256	256
F2R32	2	3200	1	1.7	512	512	256
F2R64	2	6400	1	4.2	768	768	384
F2R96	2	9600	1	7.9	1024	1024	512
F4R2	4	200	1	0.36	256	256	128
F4R4	4	400	1	0.95	256	256	128
F4R8	4	800	1	1.8	256	256	256
F4R16	4	1600	1	4.5	256	256	256
F4R32	4	3200	1	9.8	512	512	256
F4R64	4	6400	1	13.5	768	768	384
F4R96	4	9600	1	28.0	1024	1024	512

III. OVERVIEW OF THE DATABASE

Simulations were run with nominal Froude numbers (F_L) of 2 and 4, and nominal Reynolds number (Re_L) between 200 and 9600. A summary of the different cases is given in Table I, and an extensive discussion of the cases with $F_L=4$ is given in Ref. 7. Features of the simulations most relevant to the current work are briefly presented here. Initially the horizontal velocity has a periodic pattern, as evidenced by the horizontal streamfunction shown in the left hand panel of Fig. 1. With gravity acting to inhibit vertical motions, there is a strong tendency for horizontal length

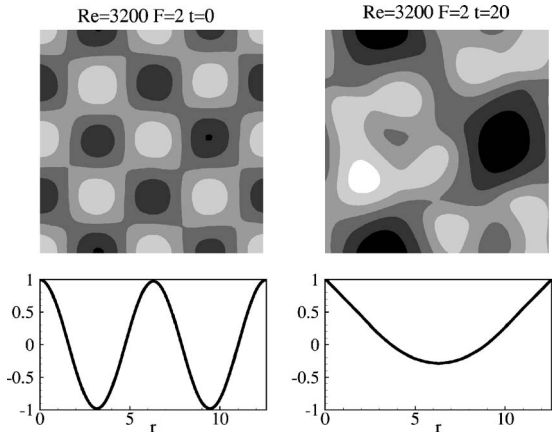

FIG. 1. Horizontal streamfunction and corresponding autocorrelation function $R(r)$ for a plane of maximum shear at time $t=0$ (left) and $t=20$ (right). $R(r)$ is defined in (6).

scales to grow. By $t=20$ the horizontal length scale has approximately doubled, as shown in the right hand panel of the same figure.

At the same time, however, there is a strong tendency for the vertical shearing of the horizontal motions to increase. This increase of the vertical shear is possibly due to the mechanism suggested by Lilly,[12] whereby the motions in adjacent horizontal layers become to some extent uncoupled. The evolution of the square of the shear, $(\partial u/\partial z)^2 + (\partial v/\partial z)^2$, averaged over horizontal planes, is shown in Fig. 2. The shear is maximum at about $t=20$ in all simulations. As turbulence in the simulations most often occurs in regions of high shear, planes of maximum shear will be considered throughout this study, unless otherwise noted. The notation $\langle\cdot\rangle_h$ denotes an average over the planes of maximum shear.

The energy of the horizontal motions is shown in Fig. 3. Initially, the vertical velocity is zero but $\rho=0$ everywhere so that the flow is not in cyclostrophic balance. As a consequence, nonzero local vertical velocity is immediately induced in the flow and there is significant cyclical transfer between kinetic and potential energy early in the simulations. By about $t=15$, the effects of the initial conditions are minor, and the average kinetic energy decreases monotonically, so

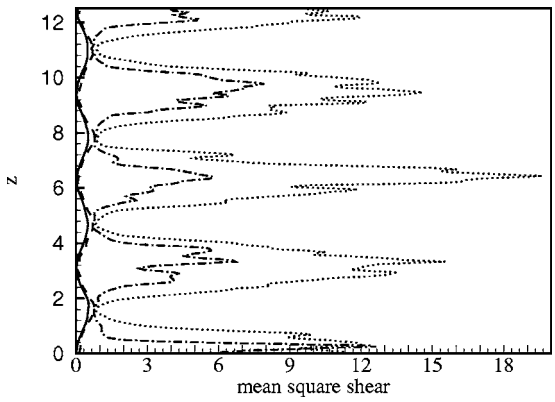

FIG. 2. Mean square vertical shearing of the horizontal velocity as a function of z for $F_\ell=2$ and $Re_\ell=3200$ at different times: $t=0$ (—), 10 (– –), 20 (–·–), and 30 (···).

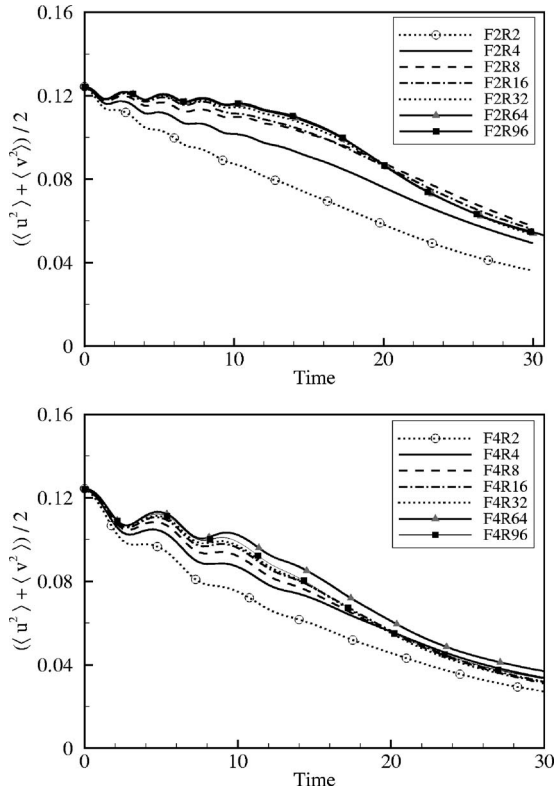

FIG. 3. Volume averaged horizontal components of kinetic energy. $F_L=2$ (upper plot), $F_L=4$ (lower plot).

that by $t=30$ the fields have less than half their initial kinetic energy. Note that the kinetic energy for all the cases, except those with a very low Reynolds number, decays at about the same rate, which suggests that the simulated flows are high Reynolds number, in the sense that they do not depend significantly on viscosity. Plots of the kinetic energy dissipation rate and energy spectra can be found in Riley and de Bruyn Kops[7]

As mentioned in the beginning of Sec. II, the simulations are motivated by experiments of decaying turbulence after a grid was dragged through a stratified fluid. While the mechanism of turbulence formation from the initial condition is certainly a topic of interest, for the purpose of studying turbulence the current simulations are most interesting in the range $15<t<25$, after the flow has reached a cyclostrophic balance and large enough energy remains for the flow to remain turbulent. Note that this range spans 2.5 nominal buoyancy periods for the $F_L=4$ case and 5 for the $F_L=2$ cases. In the remainder of the paper, we will focus on $t=20$, unless noted otherwise.

IV. ANALYSIS AND DISCUSSION

A. Vertical shear and turbulence

The vertical velocity in case F2R32 at four different times is shown in Fig. 4. The white bar in each figure connects two material points that are tracked in time. At $t=17.5$ the flow is fairly quiescent, but by $t=20$ a turbulent patch has begun to form in the vicinity of the white line. This patch continues to develop through time 22.5.

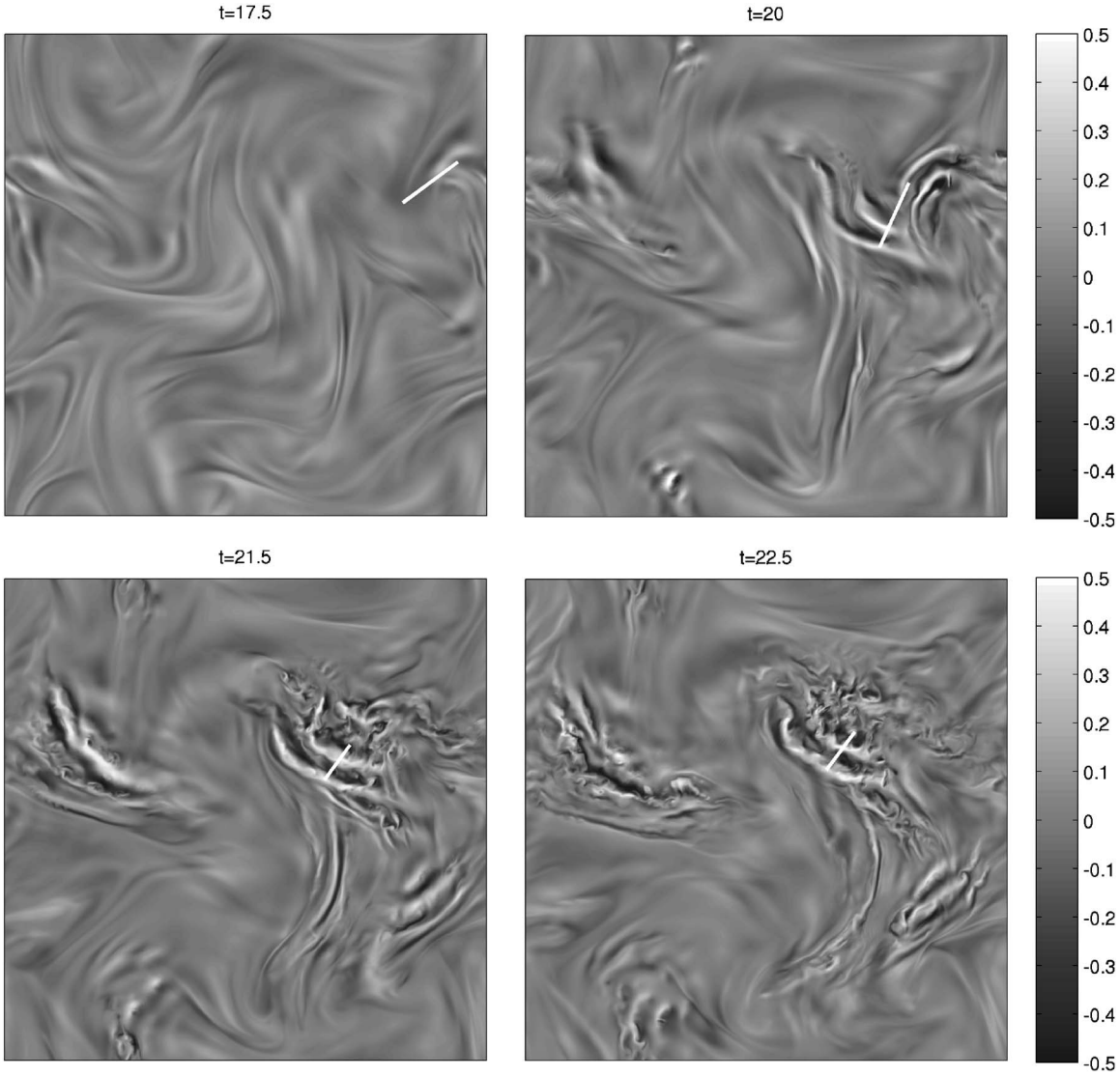

FIG. 4. A horizontal slice through the vertical velocity field at the plane of maximum shear at four different times in a Taylor-Green simulation with Froude number 2 and Reynolds number 3200. For all plots $L_x = L_y = 4 * \pi$. The white bar connects two material points that move with time. The points start in a region of relative calm, experience an instabilityand end up in a turbulent patch.

By slicing the domain vertically through the white line, the dynamics of this particular instability can be studied. In Fig. 5, the horizontal velocity in the direction of the white line is plotted for each of the four times. The figures are colored so that black indicates flow to the left and white indicates flow to the right. The gray bars above each panel in Fig. 5 correspond to the white lines in Fig. 4. At $t=17.5$ there is little shearing action in the region of the gray bar, but by $t=20$ moderate shearing has developed. By $t=21.5$ the shearing is strong, and Kelvin-Helmholtz rollups are apparent. The rollups are even more apparent in the corresponding slice through the total density field at $t=21.5$, published in Ref. 13. This type of qualitative analysis was repeated for a number of the simulation cases. While it was not always possible to find a clean Kelvin-Helmholtz rollup associated with each turbulent patch, high vertical shear accompanied the turbulence in all cases observed. Although this analysis does not provide a definitive answer, it strongly suggests vertical shear as the dominant mechanism for triggering turbulence in these simulations.

B. Intermittent turbulence

As noted in the Introduction of this paper, one of the challenges in investigating turbulence in density stratified flows is the tendency for intermittent turbulent patches to form. This requires a very large number of field samples to adequately describe flow characteristics.[14,15] Also, categorizing a flow as either laminar or turbulent is not straightforward. Wavelet analysis has proven useful for identifying turbulent structures in stably stratified flows (e.g., Refs. 16 and 17), but since the turbulence tends to be patchy and intermittent when it occurs, quantitative techniques for identifying a particular flow as "turbulent" are necessarily subjective. The

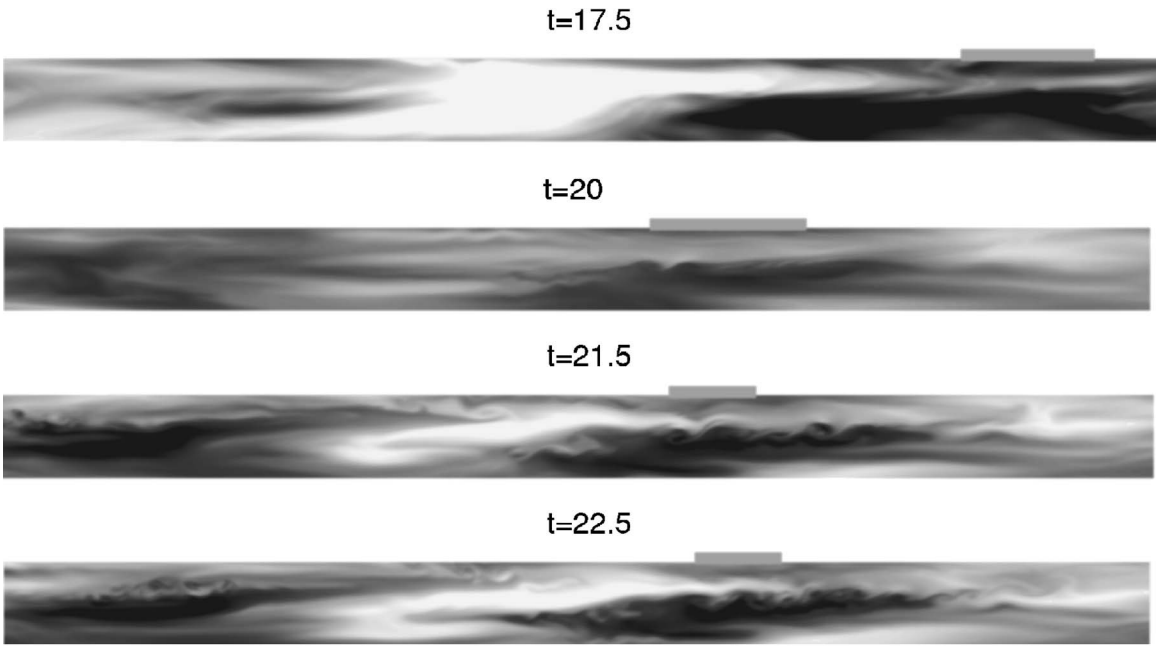

FIG. 5. The horizontal speed on vertical planes aligned with the white bar in Fig. 4. Black indicates negative and white indicates positive. The gray bar above each panel corresponds to the white bar in Fig. 4.

intermittency is pronounced in case F2R32, shown in Figs. 4 and 5. While this case is convenient for analysis because individual turbulent events can be tracked, the average buoyancy Reynolds number $\langle \mathrm{Re}_b \rangle_h$ for the plane shown is only 1.7, where

$$\langle \mathrm{Re}_b \rangle_h = \frac{\langle \epsilon \rangle_h}{\nu N^2},$$

and it might be argued that this case is not sufficiently turbulent for us to draw general conclusions about the intermittent nature of turbulence in stratified flows.

In order to understand the nature of the turbulence at higher buoyancy Reynolds numbers, we consider the plane of maximum shear for case F4R96 for which $\langle \mathrm{Re}_b \rangle_h$ is 28. The vertical velocity on the plane of maximum shear for this case is shown in the top right panel of Fig. 6, and the log of the kinetic energy dissipation rate for the same plane is shown in the lower right panel. It is apparent that while the F4R96 is more turbulent than the F2R32 case, large portions of the plane are not involved in turbulence. For instance, along the upper edge of the two right hand panels in the figure, there is a quiescent region one-third of the numerical domain width wide in which the dissipation rate is nearly four orders of magnitude smaller than in the turbulent patch just to its right.

For a comparison with unstratified isotropic homogeneous turbulence, the vertical velocity and dissipation rate for a plane taken from a simulation of the laboratory experiment by Comte-Bellot and Corrsin[18] are also shown in Fig. 6. This simulation is described in Ref. 19. In the isotropic homogeneous case, there are no large scale features evident in the dissipation rate field.

Before drawing conclusions based on Fig. 6, it is important to estimate the Reynolds numbers for each of the two simulations, since if the Reynolds number for the stratified case were much lower than that of the isotropic homogeneous case, one might expect more intermittent turbulence. In order to compare Reynolds numbers, we consider the integral length scale, computed from the autocorrelation of the velocity field in the horizontal direction, and the grid spacing, that determines the smallest scales present in the simulations. In the isotropic homogeneous case, the numerical grid has 512 points in each direction and the ratio of the numerical domain size to the integral length is about 16:1 at $x/M=98$ so that the integral length is about 32 times the grid spacing. For case F4R96, the numerical grid has 1024 points in each horizontal direction and the numerical domain is less than four times the integral length scale, which results in the integral length being about 256 times the grid spacing. So in the stratified case, the dynamic range is larger than in the isotropic homogeneous case, and more of that range is devoted to small scales. From this it can be concluded that the Reynolds number of the stratified simulation is higher than that of the isotropic homogeneous simulation, and thus the difference in behavior between the two simulations is not due to the Reynolds number in the stratified case being too low.

The intermittent nature of the turbulence raises some questions when quantitative analysis is performed. In particular, quantities involving averages of ϵ must be carefully considered since, in the current simulations, ϵ varies by nearly four orders of magnitude at large scales. This issue will be considered in more detail in the next section in the context of computing length scales.

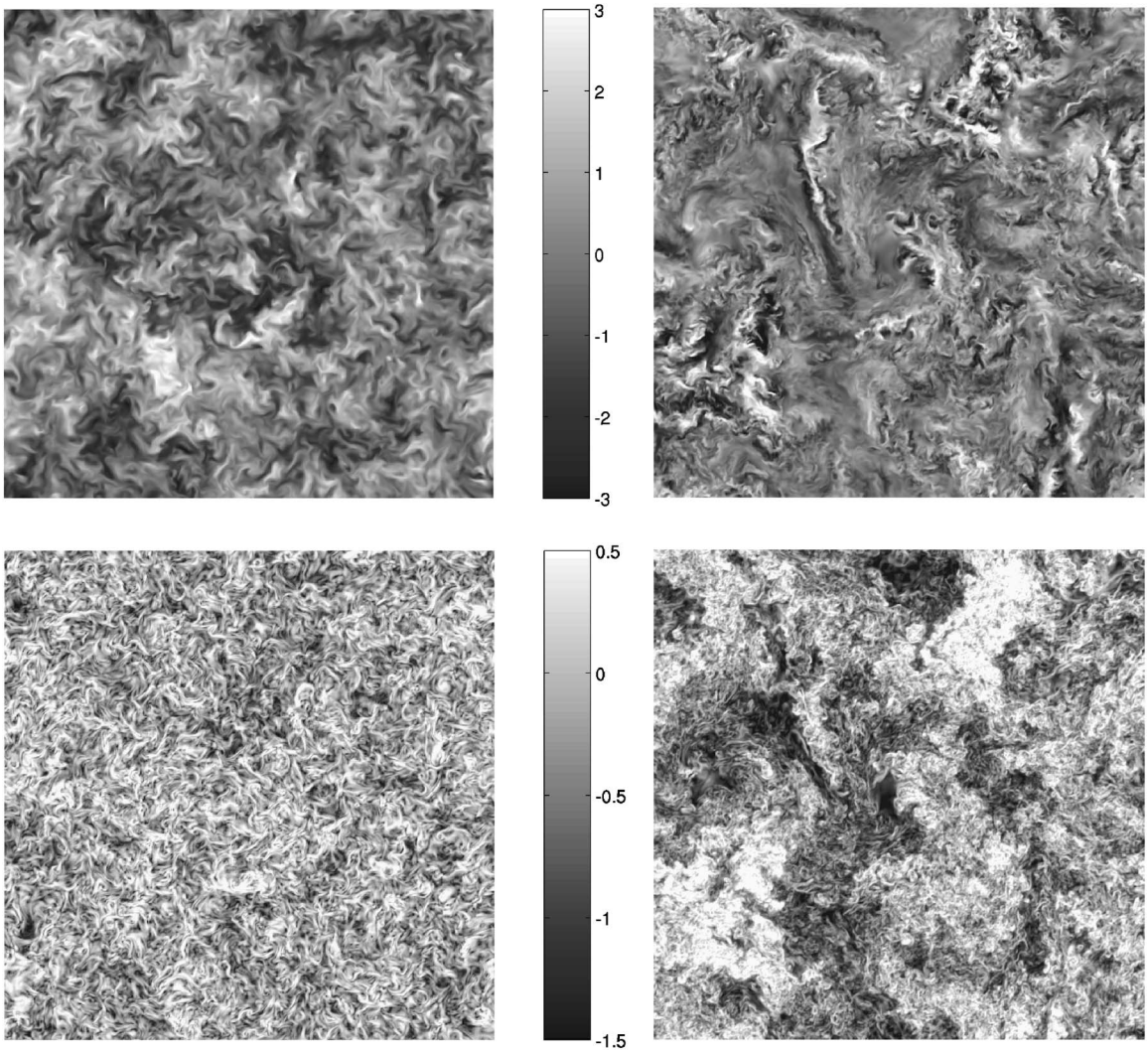

FIG. 6. Top panels: horizontal slices through the vertical velocity field. On the left, isotropic homogeneous turbulence from Ref. 19 at $x/M=98$. On the right, case F4R96 at the plane of maximum shear. In each panel, the velocity has been normalized by its rms value so that the colors in the two panels can be directly compared. Bottom panels: corresponding slices of $\log_{10}(\epsilon/\langle\epsilon\rangle_h)$.

C. Horizontal length scale

Riley and de Bruyn Kops[7] postulate a length scale, L_h, for the horizontal motions in order to define a horizontal Reynolds number, Re_h, and a horizontal Froude number, F_h, for their $F_h^2\,\mathrm{Re}_h$ scaling. How L_h is to be computed for practical use is not discussed in that paper, but their derivation of the $F_h^2\,\mathrm{Re}_h$ scaling implies that L_h can be defined in terms of u_h and ϵ (i.e., L_h is an advective length scale). Similarly, when Re_b is related to the square of a Froude number and a Reynolds number (e.g., Refs. 6 and 8), an advective length scale, u_{rms}^3/ϵ, is assumed. Therefore, it is of interest whether the advective length scale is appropriate for the large scales of motion in the current simulations.

There is a strong theoretical argument that L_h should be related to u_h (or u_{rms}) and ϵ. With appropriate spatial and temporal averaging, advection can be expected to balance the viscous dissipation rate with an advective time scale $t_a \sim L_h/u_h$. If this is the case, then

$$\frac{\partial}{\partial t}\frac{1}{2}u_h^2 \sim \epsilon \sim \frac{u_h^3}{L_h} \tag{4}$$

or $L_h \sim u_h^3/\epsilon$. While this analysis is generally accepted for theoretical estimates of the length scale, for a practical application in simulations or laboratory experiments it may not be sufficient for several reasons. First, advection of horizontal kinetic energy only balances viscous dissipation when the horizontal and vertical kinetic energies and the potential energy are in equilibrium or when a carefully chosen interval in time is used for averaging. Second, horizontal kinetic energy is convected in the vertical direction and u_h^3/ϵ varies by several orders of magnitude between planes of high and low shear. As a consequence, L_h depends strongly on the definition of the spatial averages used in its computation.

To illustrate the difficulty in using u_h^3/ϵ for analyses of the current simulations, we consider an average advective length scale

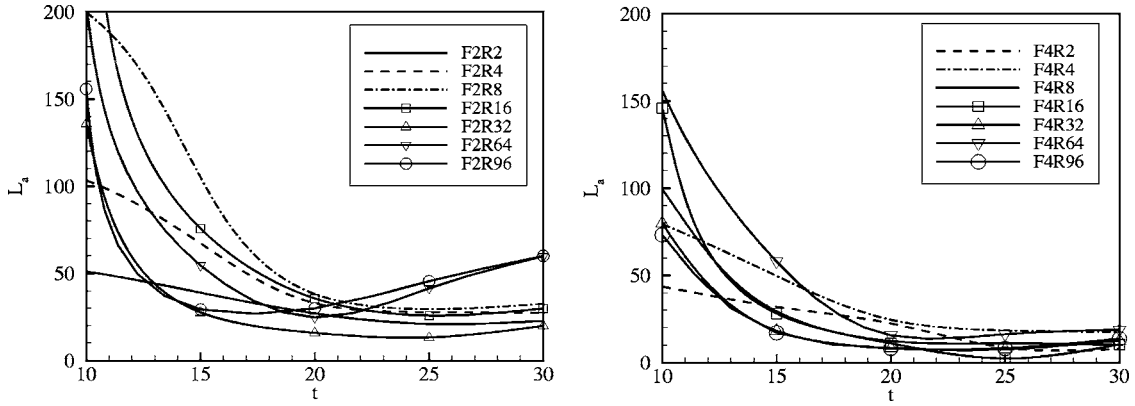

FIG. 7. Advective length scale from (5).

$$L_a = \frac{\langle u_h^3 \rangle_h}{\langle \epsilon \rangle_h}, \tag{5}$$

computed for the planes of maximum shear and plot it versus time in Fig. 7 for each of the simulation cases. Averaging in this manner is justified by the fact that most of the kinetic energy and most of its dissipation rate is associated with the planes of maximum shear, and it is in the vicinity of those planes where turbulence occurs. If the spatial average is computed over the entire domain, then the magnitude of L_a is smaller, but the trend in time is similar. Note that with the nondimensionalization given in Sec. II, the size of the numerical domain, and the fact that the domain is periodic, the maximum permissible value for the horizontal length is 2π. L_a is therefore unphysically large for most of the simulation cases. Furthermore, L_a varies significantly between the simulations and does not grow continually in time, neither of which is consistent with information about the large scales of the flow gained from the streamfunction and energy spectra. It is concluded that L_a is not useful for estimating the size of the horizontal motions in the current simulations.

In order to arrive at an appropriate length scale for use with the $F_h^2 \mathrm{Re}_h$ scaling, we consider again the underlying physical justification for that scaling (i.e., that turbulence is triggered by vertical shearing between quasihorizontal vortices). Based on this model, the appropriate length scale is the size of the horizontal vortices. From the horizontal streamfunction in Fig. 1, it is apparent that the size of these vortices increases from one quarter to one half the size of the com-

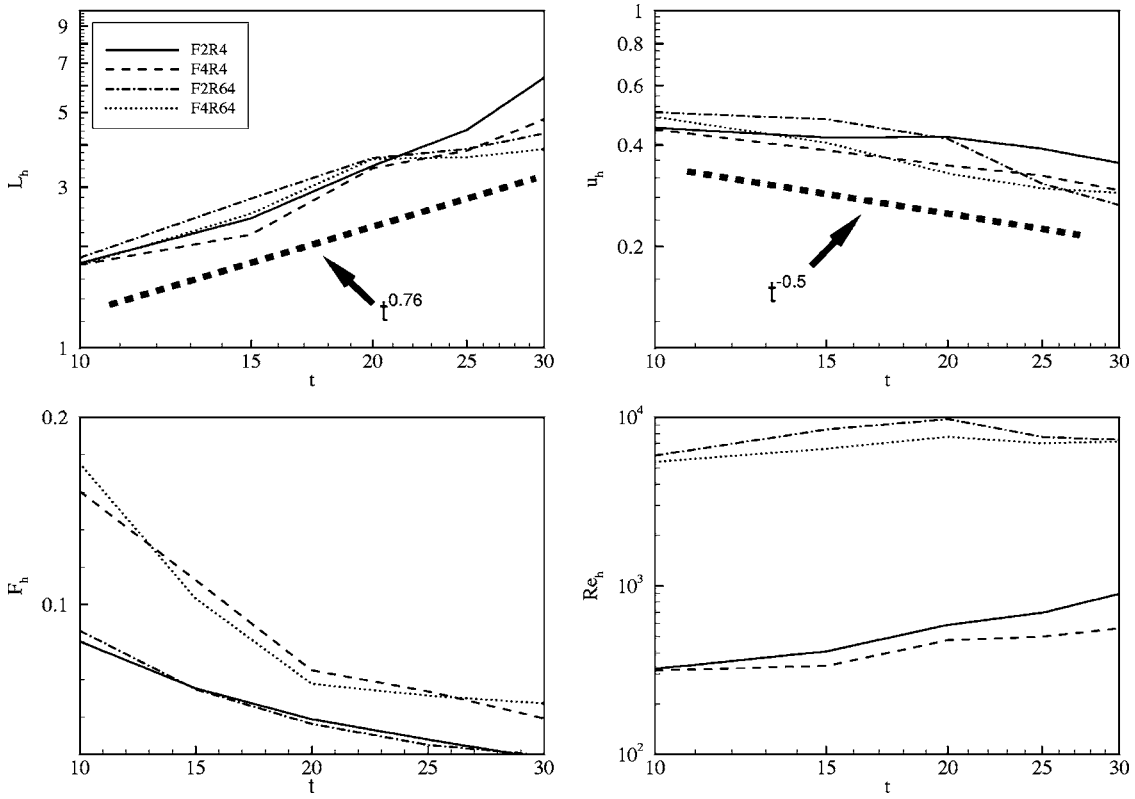

FIG. 8. L_h, u_h, F_h, and Re_h versus time for two cases with low $\langle \mathrm{Re}_b \rangle_h$ and two cases with high $\langle \mathrm{Re}_b \rangle_h$.

putational domain between $t=0$ and $t=20$. A straightforward approach to computing L_h is to relate it to the average of the autocorrelations of u in the x direction and of v in the y direction,

$$R(r) = \frac{1}{2}\frac{\langle u(x+r)u(x)\rangle_h}{\langle u\rangle_h} + \frac{1}{2}\frac{\langle v(y+r)v(y)\rangle_h}{\langle v\rangle_h}. \tag{6}$$

$R(r)$ is plotted in Fig. 1 for case F2R32 at two different times.

The horizontal length scale is defined in terms of the autocorrelation function as

$$L_h = r, \quad \text{where } R(r) = 0. \tag{7}$$

In Fig. 8, L_h from (7) is plotted versus time for cases with high and low $\langle \mathrm{Re}_b\rangle_h$. The length scale increases monotonically with time as expected and never exceeds the limiting value of 2π imposed by the initial conditions. Unlike with L_a, there is little difference in L_h between the cases, which is consistent with information gained from the streamfunction and spectra that indicate little difference in the evolution of the large scales between the different cases. This lack of dependence of L_h on stratification is also in agreement with the integral length scale results of Praud *et al.*[20] The time evolution of L_h is shown to be proportional to $t^{0.76}$, greater than the $t^{0.5}$ found from the experimental results of Voropayev and Afanasyev[21] and Praud *et al.*[20] The thick dashed line in Fig. 8 represents a line with slope 0.76. However, it should be noted that with only one third of a decade of late time data reported, the confidence interval in this relation would be large.

Also shown in Fig. 8 is the rms horizontal velocity, the horizontal Froude number, and the horizontal Reynolds number. u_H is shown to decay proportional to $t^{0.5}$. As with L_h, due to the limited range of time there is a large confidence interval. Nonetheless, using these estimates for time evolution of L_h and u_H explains the slight increase in horizontal Reynolds number with time. Also, since u_H decreases and L_h increases in time, F_h decreases in time. This data supports the theoretical argument by Riley and de Bruyn Kops[7] that stably stratified flows with no energy input will eventually enter the strongly stratified regime, even if the initial Froude number is much greater than unity.

D. Parametrization of turbulence

Having determined a suitable length scale from which to compute F_h and Re_h, we now consider the $F_h^2\,\mathrm{Re}_h$ scaling, its relationship to Re_b, and its utility for parametrizing turbulence in the simulated flows. Recall that the analysis of Riley and de Bruyn Kops[7] relates the Richardson number, Ri, to $1/F_h^2\,\mathrm{Re}_h$, so that if $F_h^2\,\mathrm{Re}_h > \mathcal{O}(1)$, then Ri can be expected to be of order one or less. Thus, a flow with $F_h^2\,\mathrm{Re}_h > \mathcal{O}(1)$ will be susceptible to Kelvin-Helmholtz instabilities and turbulence can be expected to develop. To investigate this argument, we examine the assumption that $\langle \mathrm{Ri}\rangle \sim 1/F_h^2\,\mathrm{Re}_h$ by plotting $F_h^2\,\mathrm{Re}_h$ vs $\langle \mathrm{Ri}\rangle_h$ in Fig. 9 for all the simulation cases. Here $\langle \mathrm{Ri}\rangle_h$ is the planar averaged gradient Richardson number:

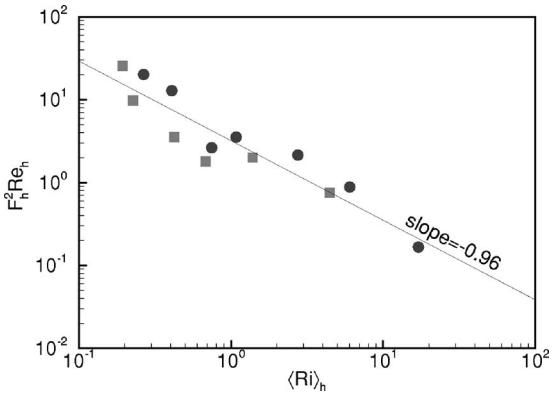

FIG. 9. $F_h^2\,\mathrm{Re}_h$ vs Ri_h. The solid line is the least-squares linear fit to the log of the quantities. The circles and squares represent the $F_L=2$ and $F_L=4$ cases, respectively.

$$\langle \mathrm{Ri}\rangle_h \equiv \frac{\dfrac{-g}{\rho_o}\left(\dfrac{\partial \rho}{\partial z} + \dfrac{d\bar{\rho}}{dz}\right)}{\left\langle \left(\dfrac{\partial u}{\partial z}\right)^2 + \left(\dfrac{\partial v}{\partial z}\right)^2 \right\rangle_h}.$$

The results are very encouraging because the relationship $\langle \mathrm{Ri}\rangle_h \sim 1/F_h^2\mathrm{Re}_h$ holds over a two decade range of values. There is some scatter in the data, but there is no tendency to deviate from the relationship, even at the extreme values of $\langle \mathrm{Ri}\rangle_h$. In fact, the stronger relationship $\langle \mathrm{Ri}\rangle_h \approx 1/F_h^2\mathrm{Re}_h$ is justified for the current simulations. The fact that $F_h^2\,\mathrm{Re}_h$ is a good estimate for the Richardson number, combined with the conclusion from Sec. IV A that shear instabilities are the major cause of turbulence in the simulations, leads us to conclude that $F_h^2\,\mathrm{Re}_h$ is a useful parameter for predicting if turbulence will occur in these flows.

It is interesting to note that the focus has been on vertical shear instability (i.e., $d\mathbf{u}/dz$). Numerical studies performed by Jacobitz and Sarkar[22] and Jacobitz[23] indicate that horizontal shear (i.e., $d\mathbf{u}/dx$ and $d\mathbf{u}/dy$) is an important factor in the production of turbulence since it does not have to overcome buoyancy forces. However, those studies were performed with a mean horizontal (and vertical) shear, whereas our simulations were performed with no applied mean shear. Furthermore, Hebert and de Bruyn Kops[24] show that in these simulated flows, vertical shear dominates horizontal shear. In addition, it is shown that as the Reynolds number is increased, the normal strain rates become more important but the horizontal shear strain rates remain small.

As noted in the Introduction, the buoyancy Reynolds number can be written in terms of a Reynolds number and the square of a Froude number. This leads to the question of whether $\langle \mathrm{Re}_b\rangle_h$ and $F_h^2\,\mathrm{Re}_h$ are related quantities, and in Fig. 10 one is plotted versus the other for all the simulation cases. It is evident that the two parametrizations are equivalent to within the scatter of the data and an order one multiplicative constant, and are in agreement with the shear flow simulations of Shih *et al.*[6] This result, in conjunction with the analysis of Riley and de Bruyn Kops[7] (Figure 9 of this paper), provides a new physical justification (i.e., shear instability) for why Re_b has proven useful for parametrizing tur-

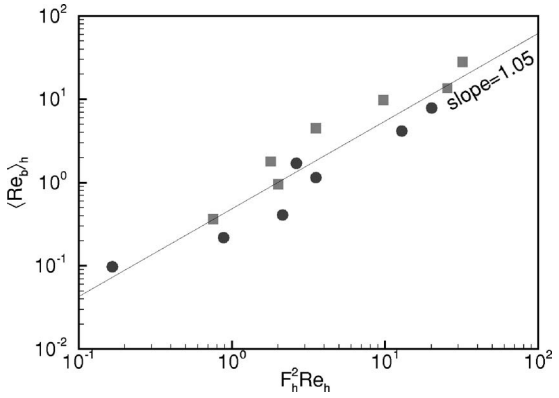

FIG. 10. $\langle \mathrm{Re}_b \rangle_h$ vs $F_h^2 \mathrm{Re}_h$. The solid line is the least-squares linear fit to the log of the quantities. The circles and squares represent the $F_L=2$ and $F_L=4$ cases, respectively.

bulence in stably stratified flows. This alternative justification may help in understanding the conditions under which Re_b can be used to parametrize turbulence, and how the parametrization might be improved.

In addition to providing an alternative physical explanation for the occurrence of turbulence under stable stratification, the $F_h^2 \mathrm{Re}_h$ scaling has several attractive features compared with Re_b. At the theoretical level, it involves two dimensionless groups, which is the number predicted for this problem by the Buckingham Pi theorem. This suggests that turbulence parametrization be considered in the two dimensional Froude-Reynolds number space, which is likely to be a more intuitive method of describing the flow conditions, rather than in the one dimensional domain of a modified Reynolds or modified Froude number. At the practical level for numerical and laboratory experimentalists, $F_h^2 \mathrm{Re}_h$ can be used *a priori* to estimate if a flow can be expected to be sufficiently turbulent to be interesting for understanding oceanic and atmospheric flows.

V. CONCLUSIONS

A series of high-resolution direct numerical simulations is used to investigate turbulence in stably stratified flows. The simulated flows are dominated by vortical modes and decay in time, since there is no input of energy from the mean flow. In this regime, the Froude number decreases and the Reynolds number increases in time so that a strongly stratified flow with turbulence eventually develops, except when the initial Reynolds number is extremely low. The predominant cause of turbulence in the simulations is Kelvin-Helmholtz instabilities that result when the flow organizes itself into quasihorizontal vortices that are weakly coupled in the vertical direction.

This observation that shear instabilities are the primary trigger for turbulence in the simulations supports the theoretical derivation of the $F_h^2 \mathrm{Re}_h$ parametrization developed in Ref. 7, namely, that $1/F_h^2 \mathrm{Re}_h$ is related to the Richardson number, so when $F_h^2 \mathrm{Re}_h > \mathcal{O}(1)$, then turbulence can be expected. To test this hypothesis, the length scale, L_h, on which F_h and Re_h are based, is defined as the correlation length of the horizontal velocity. When this definition is used it is observed that L_h, F_h, and Re_h all evolve in time consistently with theoretical predictions for all the simulation cases. Furthermore, $1/F_h^2 \mathrm{Re}_h \approx \mathrm{Ri}$ over a two decade span of Richardson numbers. This result encourages the thought that $F_h^2 \mathrm{Re}_h$ can be used *a priori* to estimate if a laboratory or simulated flow will involve considerable turbulence, provided that the correlation length of the horizontal velocity can be estimated from the initial and boundary conditions for the flow.

Finally, $F_h^2 \mathrm{Re}_h$ is compared with the buoyancy Reynolds number for all the simulation cases, and it is found that the two quantities are about the same to within the scatter of the data and an order one multiplicative constant. While Re_b is traditionally defined as the ratio of the overturning length scale to the viscous length scale, the fact that $F_h^2 \mathrm{Re}_h \sim \mathrm{Re}_b$ suggests that a shear-based argument might be used to better explain why Re_b has proven to be a useful parametrization. Also, since $F_h^2 \mathrm{Re}_h$ involves the number of dimensionless groups predicted by dimensional analysis, it encourages considering turbulence in stratified flows as occurring when the Froude and Reynolds numbers are in some region of the two-dimensional Froude-Reynolds number space rather than when the buoyancy Reynolds number is above some transition value.

ACKNOWLEDGMENTS

The authors thank Professor Jim Riley for numerous discussions on the topics presented in this paper. This research is funded by the U.S. Office of Naval Research, Grant No. N00014-04-1-0687, managed by Dr.. R. D. Joslin. Grants of high performance computer time were provided by the Arctic Region Supercomputing Center and the Army Engineer Research and Development Center.

[1] C. H. Gibson, in *Marine Turbulence*, edited by J. C. Nihous (Elsevier, Amsterdam, 1980), pp. 221–257.
[2] M. C. Gregg, "Diapycnal mixing in the thermocline–a review," J. Geophys. Res. [Oceans] **92**, 5249 (1987).
[3] W. D. Smyth and J. N. Moum, "Length scales of turbulence in stably stratified mixing layers," Phys. Fluids **12**, 1327 (2000).
[4] J. Imberger and B. Boashash, "Application of the winger-ville distribution to temperature gradient microstructure: A new technique to study small-scale variations," J. Phys. Oceanogr. **16**, 1997 (1986).
[5] D. C. Stillinger, K. N. Helland, and C. W. V. Atta, "Experiments on the transition of homogeneous turbulence to internal waves in a stratified fluid," J. Fluid Mech. **131**, 91 (1983).
[6] L. H. Shih, J. R. Koseff, G. N. Ivey, and J. H. Ferziger, "Parameterization of turbulent fluxes and scales using homogeneous sheared stably stratified turbulence simulations," J. Fluid Mech. **525**, 193 (2005).
[7] J. J. Riley and S. M. de Bruyn Kops, "Dynamics of turbulence strongly influenced by buoyancy," Phys. Fluids **15**, 2047 (2003).
[8] G. N. Ivey and J. Imberger, "On the nature of turbulence in a stratified fluid.1. the energetics of mixing," J. Phys. Oceanogr. **21**, 650 (1991).
[9] A. M. Fincham, T. Maxworthy, and G. R. Spedding, "Energy dissipation and vortex structure in freely decaying, stratified grid turbulence," Dyn. Atmos. Oceans **23**, 155 (1996).
[10] R. M. Kerr, "Higher-order derivative correlations and the alignment of small-scale structures in isotropic turbulence," J. Fluid Mech. **153**, 31 (1985).
[11] J. P. Boyd, *Chebyshev and Fourier Spectral Methods* (Dover, New York, 2001).
[12] D. K. Lilly, "Stratified turbulence and the mesoscale variability of the atmosphere," J. Atmos. Sci. **40**, 749 (1983).
[13] S. M. de Bruyn Kops, J. J. Riley, and K. B. Winters, in *Reynolds Number Scaling in Turbulent Flow* (Kluwer, Dordrecht, 2003).
[14] M. A. Baker and C. H. Gibson, "Sampling turbulence in the stratified

ocean: statistical consequences of strong intermittency," J. Phys. Oceanogr. **17**, 1817 (1987).
[15]C. H. Gibson, "Buoyancy effects in turbulent mixing: Sampling turbulence in the stratified ocean," AIAA J. **19**, 1394 (1981).
[16]M. Farge, "Wavelet transforms and their applications to turbulence," Annu. Rev. Fluid Mech. **24**, 395 (1992).
[17]G. Katul and B. Vidakovic, "Identification of low-dimensional energy containing/flux transporting eddy motion in the atmospheric surface layer using wavelet thresholding methods," J. Atmos. Sci. **55**, 377 (1998).
[18]G. Comte-Bellot and S. Corrsin, "Simple Eulerian time correlation of full and narrow-band velocity signals in grid-generated, 'isotropic' turbulence," J. Fluid Mech. **48**, 273 (1971).
[19]S. M. de Bruyn Kops and J. J. Riley, "Direct numerical simulation of laboratory experiments in isotropic turbulence," Phys. Fluids **10**, 2125 (1998).
[20]O. Praud, A. M. Fincham, and J. Sommeria, "Decaying grid turbulence in a strongly stratified fluid," J. Fluid Mech. **522**, 1 (2005).
[21]S. I. Voropayev and Y. D. Afanasyev, "Two-dimensional vortex-dipole interactions in a stratified fluid," J. Fluid Mech. **236**, 665 (1992).
[22]F. G. Jacobitz and S. Sarkar, "The effect of nonvertical shear on turbulence in a stably stratified medium," Phys. Fluids **10**, 1158 (1998).
[23]F. G. Jacobitz, A comparison of the turbulence evolution in a stratified fluid with vertical or horizontal shear, J. Turbul. **3**, 1–16 (2002).
[24]D. A. Hebert and S. M. de Bruyn Kops, "Relationship between vertical shear rate and kinetic energy dissipation rate in stably stratified flows," Geophys. Res. Lett. **33**, L06602 (2006).